On phase feedback for nonlinear MEMS resonators

R. M. C. Mestrom, R. H. B. Fey, H. Nijmeijer
Department of Mechanical Engineering, Dynamics and Control Group
Technische Universiteit Eindhoven
Eindhoven, the Netherlands
Email: r.m.c.mestrom@tue.nl

***Abstract*— In oscillator circuits, a resonator acts as a frequency selective network. Nonlinearities in the resonator may influence oscillator performance and may limit the signal to noise ratio. In this paper, a phase feedback approach for increasing the signal to noise ratio in MEMS resonators is investigated. The approach consists of fine-tuning the frequency at which the resonator oscillates by means of setting the oscillation phase condition in the amplifier of the oscillator circuit. The approach is explained for a nonlinear Duffing resonator, which is representative for certain types of MEMS resonators. Here, this approach is applied to a nonlinear clamped-clamped beam MEMS resonator. On simulation level, closed-loop phase feedback yields an increase in S/N-ratio of several decades compared to the open-loop system. Furthermore, optimal operation points for oscillator circuits incorporating a nonlinear resonator can be defined.**

I. Introduction

Micro-electromechanical silicon resonators provide an interesting alternative for quartz crystals as accurate timing devices in oscillator circuits for modern data and communication applications [1]. Their compact size, feasibility of integration with IC technology and low cost are major advantages. In oscillator circuits, nonlinearities in resonators influence oscillator performance. Conventional quartz crystal resonators are not driven into nonlinear regimes, since the rather bulky quartz crystal units can store sufficient energy for oscillation while remaining linear. However, MEMS resonators inherently can store less energy, due to their smaller size [2]. For this reason, they have to be driven into nonlinear regimes.

In this paper, an approach for coping with nonlinearities of MEMS resonators in oscillator circuits will be investigated. For this purpose, first, in Section II, the principle and oscillation conditions for oscillator circuits will be explained. Next, in Section III, the approach for coping with nonlinearities in resonators will be explained by introducing the principle of phase feedback (Section III-A). Subsequently, this approach will be applied to a clamped-clamped beam MEMS resonator in Section III-B. Simulation results for this resonator will be presented in Section IV and, finally, some conclusions will be drawn in Section V.

II. Oscillator Circuits

An oscillator is a circuit that produces a periodic output signal with a high spectral purity. A schematic representation of an oscillator is depicted in Fig. 1. Virtually all oscillators may be considered to consist of two essential parts [3], [4]. an amplifier (or gain circuit) and a resonator, which acts as a frequency selective network. The amplifier portion usually consists of one or more active devices (hence, the power supply) and the necessary biasing networks. It may also contain other elements for band limiting, impedance matching and gain control. The resonator determines the frequency and stability of the generated signal. It can be an LC circuit, a quartz crystal or a MEMS resonator, which is able to vibrate at a specific angular frequency Ω. Next to the resonator, some other parts might be present, like variable capacitors for tuning.

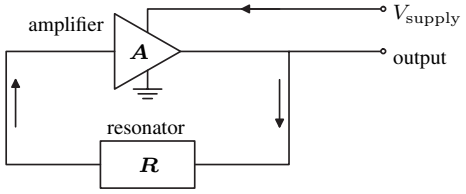

Fig. 1. Basic oscillator circuit, consisting of an amplifier $\boldsymbol{A}$ and a resonator or feedback circuit $\boldsymbol{R}$.

From Fig. 1, it can be seen that the output of the resonator is fed back into the amplifier. If this happens with the correct amplitude and phase, sustained oscillations may occur [5]. Suppose the amplifier has a voltage gain $\boldsymbol{A}$ and the resonator has a voltage ratio $\boldsymbol{R}$. Next, consider for the moment that a signal $\boldsymbol{e}$ exists at the input of the amplifier. The signal appearing at the output terminal of the amplifier will be $\boldsymbol{Ae}$. When this signal is transferred through the resonator, the 'new' amplifier input reads $\boldsymbol{e}' = \boldsymbol{RAe}$. When $\boldsymbol{e}'$ has the same angular frequency and phase as $\boldsymbol{e}$ and $|\boldsymbol{e}'| \geq |\boldsymbol{e}|$, the circuit will oscillate. In general, both $\boldsymbol{A}$ and $\boldsymbol{R}$ will be complex functions of the angular oscillation frequency Ω. By writing their complex gains as $\boldsymbol{R} = G_R(\Omega)\exp(j\psi_R(\Omega))$ and $\boldsymbol{A} = G_A(\Omega)\exp(j\psi_A(\Omega))$, the total gain of the oscillator circuit becomes:

$$\boldsymbol{RA} = G_R(\Omega)G_A(\Omega)\exp(j(\psi_R(\Omega)+\psi_A(\Omega))). \quad (1)$$

Here, $G_R(\Omega)$ and $G_A(\Omega)$ are the magnitudes of the resonator and amplifier gain, respectively and $\psi_R(\Omega)$ and $\psi_A(\Omega)$ represent the corresponding phase shifts. The requirements for oscillation can now be formulated as follows:

$$\psi_R(\Omega)+\psi_A(\Omega) = 2n\pi, \qquad n = 0, 1, 2, \ldots \quad (2)$$

$$G_R(\Omega)G_A(\Omega) \geq 1. \quad (3)$$

The first condition (2) states that the total phase shift around the oscillator must be an integral multiple of 2π radians. The

1-4244-0647-1/07/$20.00 ©2007 IEEE

oscillation frequency is determined by this condition. At this frequency, the second condition (3) states that the magnitude of the amplifier gain must be sufficient to compensate for the resonator losses. In other words, the loop gain must be greater than unity in order for oscillations to build up. As a result, the signal level in the loop will continue to increase until the amplifier gain is reduced, either by nonlinearities in the active elements or by some automatic level-control method. Eventually, in steady-state, (3) becomes an equality.

When the oscillator is initially turned on, the only signal present in the circuit is ('white' or thermal) electrical noise associated with the components (mainly the active ones) in the circuit. The frequency component of the noise whose frequency satisfies the phase requirement for oscillation is propagated around the loop with increasing amplitude, until the steady-state situation with sustained oscillation is reached. The rate of increase of the signal amplitude depends on the excess gain of the loop.

III. Phase Feedback

A. Principle of Phase Feedback

The small size of MEMS resonators makes that they often have to be driven into nonlinear regimes. Nonlinear effects include, but are not limited to, geometric nonlinearities due to (relatively) large vibration amplitudes [2], [6], [7], electrostatic nonlinearities due to capacitive excitation and detection [2], and material nonlinearities like higher-order elastic effects [8]. These nonlinear effects may effectively be described by a simplified or lumped model with a Duffing-like structure, see [2]. Therefore, without loss of generality, the principle of phase feedback will be explained for a Duffing system, which is one of the most simple forms of a nonlinear resonator. The differential equation for the forced Duffing system is given as [7]:

$$m\ddot{x} + b\dot{x} + k_0 x + k_2 x^3 = F_0 \cos \Omega t, \tag{4}$$

where parameters m, b, k_0 and k_2 denote mass, damping, linear stiffness and cubic stiffness parameters, respectively. The forcing has an amplitude F_0 and an angular excitation frequency Ω. The Duffing oscillator will prove to be representative for certain types of MEMS resonators, as will be discussed in Section III-B. By introducing parameters

$$\omega_0 = \sqrt{\frac{k_0}{m}}, \quad \xi = \frac{b}{2\sqrt{k_0 m}}, \quad \gamma = \frac{k_2}{k_0}\omega_0^2, \text{ and } \quad q = \frac{F_0}{m}, \tag{5}$$

(4) can be rewritten as

$$\ddot{x} + 2\xi\omega_0\dot{x} + \omega_0^2 x + \gamma x^3 = q \cos \Omega t. \tag{6}$$

An approximate solution to the response of the Duffing system to a resonant excitation ($\Omega \approx \omega_0$) can be obtained by applying the method of multiple scales [7], [9]. This method can only be applied to weakly nonlinear systems. Therefore, a small bookkeeping parameter $\varepsilon \ll 1$ will be introduced to indicate that the nonlinearity is weak compared to linear terms. For the case of resonant excitation, as considered here, also the excitation and damping terms are scaled:

$$\ddot{x} + \omega_0^2 x = \varepsilon(q \cos \Omega t - 2\xi\omega_0\dot{x} - \gamma x^3). \tag{7}$$

Here, the equation has been arranged such that the left-hand side constitutes a linear undamped system. The method of multiple scales allows for the steady-state solution of (7) to be written as [7]:

$$x = a\cos(\Omega t - \psi) + \varepsilon\frac{\gamma}{32\omega_0^2}a^3\cos(3(\Omega t - \psi)) + \mathcal{O}(\varepsilon^2), \tag{8}$$

where a is given by the solution to the so-called frequency response equation

$$q^2 = a^2\left[(2\xi\omega_0^2)^2 + \left(\frac{3}{4}\gamma a^2 - 2\sigma\omega_0^2\right)^2\right] \tag{9}$$

and the phase ψ results from

$$\tan\psi = \frac{-\xi\omega_0}{\sigma - \frac{3\gamma}{8\omega_0}a^2}. \tag{10}$$

As mentioned before, parameter ε in (7) and (8) is a small bookkeeping parameter, which serves to indicate the order of approximation and σ (see (9) and (10)) is the frequency detuning $\sigma = \Omega - \omega_0$. Furthermore, stability of solutions (a, ψ) holds if

$$\left(\sigma - \frac{3\gamma}{8\omega_0}a^2\right)\left(\sigma - \frac{9\gamma}{8\omega_0}a^2\right) + (\xi\omega_0)^2 < 0. \tag{11}$$

By using (9)–(11), amplitude-frequency curves and phase-frequency curves can be approximated based on the fundamental harmonic term in (8). These curves are nonlinear equivalents to the magnitude and phase curves of the Bode diagram. This is depicted in Fig. 2 for some specific parameter values $\omega_0 = 2\pi$ rad/s, $\xi = 0.005$, $\gamma = -5$ m^{-2}s^{-2}, and $q = 0.4$ m/s^2. Stability of the periodic solutions has been determined by (11) and is also indicated.

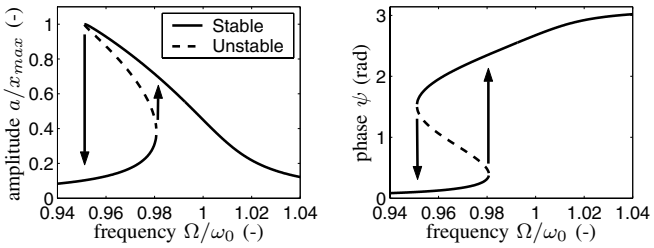

Fig. 2. Amplitude-frequency and phase-frequency curve for the Duffing resonator (linear natural frequency is ω_0).

Figure 2 contains the amplitude-frequency curve (left), which depicts the normalised amplitude (a/x_{max}) of oscillation versus frequency. In practice, jumps will be observed in the steady-state nonlinear dynamic behaviour of the resonator when one sweeps up and down through the fundamental resonance region. These jumps are also indicated in Fig. 2 by the arrows. This effect is also known as frequency hysteresis. The right part shows the corresponding phase-frequency curve.

Recall that both curves are based on the assumption that the system response (8) may be approximated by a linear response (only the first harmonic term in (8)). Otherwise, the term phase has no meaning for nonlinear systems. For the relatively large value of the nonlinearity used here ($\gamma = -5\ \mathrm{m^{-2}s^{-2}}$), this may be only a very crude approximation, since the Duffing resonator may no longer be considered as a weakly nonlinear system.

For the approximation, given in (8), the phase can be calculated by (10). From the figure, it can be seen that the phase changes by π rad over the resonance peak, similar to the phase change in a linear system. Finally, note from Fig. 2 that both the amplitude a and the phase ψ are *not* single-valued functions of the excitation frequency.

In order to cope with resonator nonlinearities in an oscillator environment, a technique, described in [10], [11], will be explained. This will be called *phase feedback*. Consider the phase-frequency curve in Fig. 2 (right) again. Although the phase is not a single-valued function of the excitation frequency, this is the case the other way around. In other words, *frequency is a single valued function of phase*, that is $\psi = \psi(\Omega/\omega_0)$. This is depicted in Fig. 3. This observation

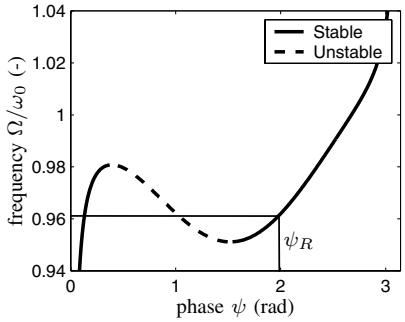

Fig. 3. Frequency-phase curve for Duffing resonator.

is suitable for oscillator applications, since the resonator and amplifier together have to satisfy gain and phase requirements (2)–(3). As a result, the frequency at which the resonator oscillates can be fixed by setting the amplifier part of the oscillator circuit to a suitable phase condition. For instance, the resonator can be forced to oscillate at frequency of $\Omega \approx 0.96\omega_0$ with a phase of $\psi_R = 2$ rad (see Fig. 3), by setting the amplifier phase to $\psi_A = 2\pi - \psi_R$, see (2). In this way, the resonator can be set to oscillate at a high-amplitude solution (at the peak in the left part of Fig. 2).

It will become clear in Section IV that, with phase feedback, it can even operate on the unstable part of the curve. Moreover, a resonator phase near $\psi_R = \pi/2$ rad not only results in high-amplitude resonator oscillations, but also in small sensitivity of the oscillation frequency to changes in phase. Namely, the frequency Ω/ω_0 is not very sensitive for changes in ψ, since the frequency-phase function is (almost) horizontal in the region around $\psi = \pi/2$ rad, see Fig. 3. The method described above has been used in a recently developed sensitive magnetometer, described in [12].

B. Application to a MEMS Resonator

The phase feedback approach, described in the previous section, will be applied to a clamped-clamped beam MEMS resonator. The model for the resonator has a Duffing-like structure, and is able to describe measured nonlinear dynamical behaviour rather well [13].

A schematic representation of the clamped-clamped beam resonator is depicted in Fig. 4. Its characteristic vibration shape is shown in Fig. 4(a). Due to out-of-plane vibration, the resonator is often called a flexural resonator. The actuation of the resonator is realised by means of a dc (V_{dc}) and an ac (V_{ac}) voltage component, which are applied to the electrodes of the resonator by means of bias tees, see Fig. 4(b). Note that the dc voltage V_{dc} is applied to both electrodes of the beam, whereas the ac voltage is applied to a single electrode.

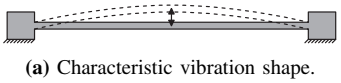

(a) Characteristic vibration shape.

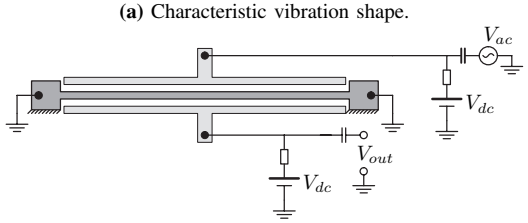

(b) Actuation by a dc and an ac voltage component.

Fig. 4. Schematic layout of a clamped-clamped beam resonator.

A lumped 1DOF model, describing the dynamics of the MEMS resonator is [13]:

$$m\ddot{x} + b\dot{x} + k(x)x = F_e(x,t), \tag{12}$$

where m, b and $k(x)$ are the lumped mass, damping and nonlinear stiffness of the system, respectively. Since the beam is excited over the total beam length (see Fig. 4), x is some characteristic displacement measure for the beam, vibrating in the first mode. Furthermore, $\dot{x}$ and $\ddot{x}$ denote the first and second time derivative of x, respectively. The electrostatic force $F_e(x,t)$ is given by:

$$F_e(x,t) = \frac{1}{2}\frac{C_0 d_0}{(d_0 - x)^2}V_1^2(t) - \frac{1}{2}\frac{C_0 d_0}{(d_0 + x)^2}V_2^2, \tag{13}$$

where C_0 is the capacitance over the gap when $x = 0$ and d_0 is the corresponding initial gap width. V_1 and V_2 denote the applied voltages on the electrodes and are written as

$$V_1(t) = V_{dc} + V_{ac}\sin(2\pi f t), \qquad V_2 = V_{dc}, \tag{14}$$

where V_{dc} is the so-called bias voltage, and V_{ac} and f are the amplitude and frequency of the ac voltage, respectively. The nonlinear stiffness function, including terms up to fourth order is written as [13]:

$$k(x) = k_0 + k_1 x + k_2 x^2 + k_3 x^3 + k_4 x^4, \tag{15}$$

where k_0 is the stiffness parameter in the linear part of the spring force and k_1, k_2, k_3 and k_4 denote the stiffness parameters in the nonlinear part of the spring force.

The linear natural frequency of the clamped-clamped beam resonator equals $f_0 = \omega_0/(2\pi) = 1/(2\pi)\sqrt{k_0/m}$. Due to electrostatic actuation, this frequency will change slightly to $f_{0,e} = 1/(2\pi)\sqrt{k_{0,e}/m}$, where stiffness $k_{0,e}$ equals k_0 offset by a V_{dc}^2-term: $k_{0,e} = k_0 - 2C_0V_{dc}^2/d_0^2$.

An oscillator circuit model including the nonlinear MEMS resonator (12)–(15) has been implemented numerically in order to be able to perform closed-loop simulations with phase feedback. The schematic structure is depicted in Fig. 5. The

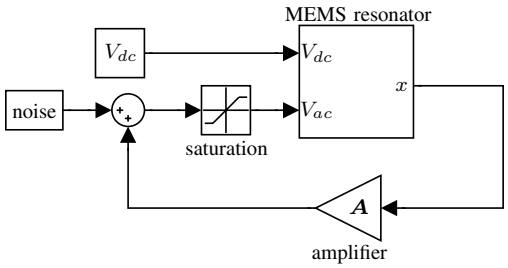

Fig. 5. Block diagram of the oscillator circuit with the MEMS resonator.

oscillator circuit can be seen to consist of the MEMS resonator and an amplifier. The resonator is driven by a bias voltage V_{dc} and an input voltage $V_{in} = V_{ac}$ on the resonator ac input. The oscillator is self-starting due to noise. The resonator output, displacement x, is amplified and fed back into the resonator. The input to the MEMS resonator is limited in amplitude by a saturation function. Otherwise, the oscillation amplitude would grow excessively. The oscillator circuit has to satisfy two conditions (2)–(3) in order for oscillations to sustain. Therefore, the amplifier consists of two parts, a gain and a phase change. The latter is implemented by means of a transport delay with a delay time of $\Delta t_A = \psi_A/(2\pi f_{0,e})$, where ψ_A denotes the required amplifier phase. In the next section, results for phase feedback with the MEMS resonator will be discussed.

IV. Results

For all results listed in this section, the set of parameter values listed in table I has been used [13]. The value of V_{ac} should be interpreted as the saturation level in the saturation block in Fig. 5. From these parameter values, the fundamental frequency can be calculated to be $f_0 = 12.945$ MHz. Furthermore, the amplitude-frequency curve has been calculated numerically using AUTO [14] and is depicted in Fig. 6. The response is similar to that of the Duffing resonator (Fig. 2).

Next, the effect of phase feedback on the resonator output is investigated. A typical result is shown in Fig. 7, where Fig. 7(a) shows the resonator output without feedback and Fig. 7(b) shows the output signal in case of feedback. Here, the amplifier gain is chosen such that oscillations will swing up. For now, a rather large gain of $\mathcal{O}(10^9)$ V/m is used, which can be motivated by the fact that the very small position x is used for feedback. The influence of the gain on the phase feedback results is still a topic of further research.

TABLE I

Numerical values for the model parameters.

Parameter	Value	Unit
m	2.275×10^{-13}	kg
b	2.721×10^{-9}	kg/s
k_0	1.505×10^{3}	N/m
k_1	0.0	N/m^2
k_2	-6.200×10^{15}	N/m^3
k_3	0.0	N/m^4
k_4	1.200×10^{30}	N/m^5
d_0	0.330×10^{-6}	m
C_0	0.185×10^{-15}	F
V_{dc}	70.0	V
V_{ac}	0.180	V

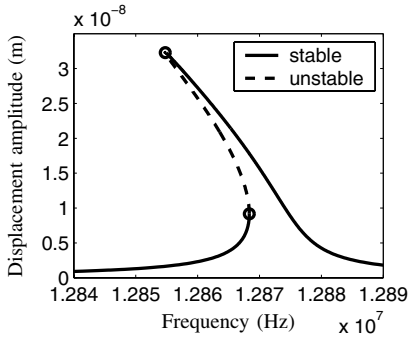

Fig. 6. Amplitude frequency curve for the MEMS resonator and the parameter values listed in Table I.

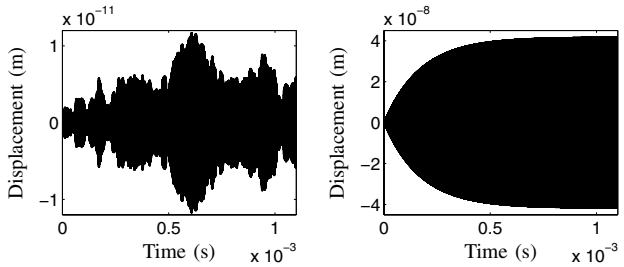

Fig. 7. Input (a) and output (b) of MEMS resonator without feedback.

The amplifier phase is set to $\psi_A = 2\pi - \pi/2$ rad to force the resonator to operate at $\psi_R = \pi/2$ rad. From Fig. 7(b), it can be seen that it takes some time for the resonator to reach its steady state. The reason for this is the very low damping parameter of the system. The Q-factor of the system is $Q = 1/(2\xi) = \sqrt{k_{0,e}m}/b = 6.8 \times 10^3$. In steady state, the oscillator output is periodic. The autopower spectra of the output signals with and without feedback have been calculated and are depicted in Fig. 8. Here, the resonator displacement output x is used in order to be able to compare the situation with and without feedback. In practice, however, the amplifier output would be used (see Fig. 1). From Fig. 8, it can be seen that the output of the circuit with feedback has a much better S/N-ratio than

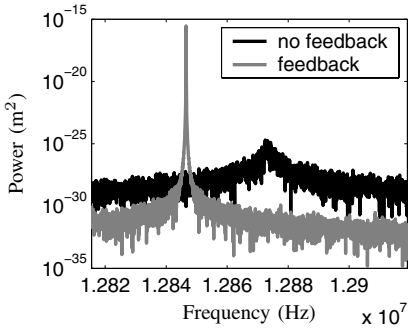

Fig. 8. Autopower spectrum of the resonator output with and without phase feedback.

for the circuit without feedback. Namely, the peak near the fundamental frequency is several decades higher, and the base noise level is a little lower in the feedback case.

Furthermore, it can be seen that the fundamental frequency in the feedback case is slightly lower than in the case without feedback. This is the result of the phase-dependence of the oscillation frequency (see Fig. 3), where a functional relation between frequency and phase exists. In order to investigate this behaviour, a simulation study has been performed in which the requested phase ψ_R of the MEMS resonator is varied between 0 and π rad. For each phase ψ_R, and, consequently, for each amplifier phase $\psi_A = 2\pi - \psi_R$, the fundamental frequency in the output is determined. This is depicted in Fig. 9(a). This figure is qualitatively similar to Fig. 3. The

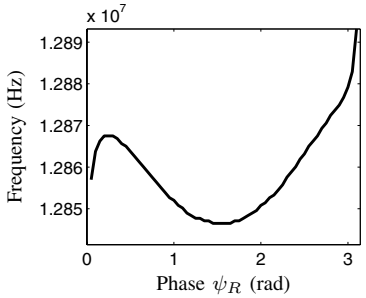

(a) frequency-phase curve.

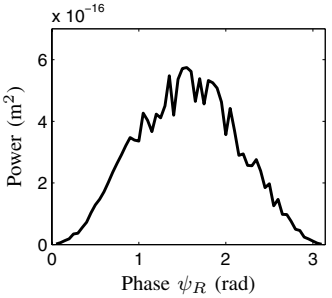

(b) power-phase curve.

Fig. 9. Frequency-phase curve (a) and power-phase curve (b) for the feedback circuit with the MEMS resonator.

minimum of the analytical curve for the Duffing system is present at $\psi = \pi/2$ rad, which corresponds very well with the minimum in Fig. 9(a). The region to the left of the minimum ($0.5 \leq \psi_R \leq \pi/2$ rad) would correspond to the unstable part of the open-loop frequency-phase curve (see Fig. 3). However, in case of phase feedback, the unstable part is stabilised.

Although the analytical approximation in Section III-A is only valid for weakly nonlinear systems, the phase feedback concept still works very well for the stronger nonlinear MEMS resonator investigated here. The concept limits are still a topic of further research.

For oscillator applications, a large S/N-ratio in the circuit output is desired. Required for this is a high output power and low noise. Output power is a measure for the desired fundamental signal content. Furthermore, the noise level even decreases in case of feedback (see Fig. 8). The power at the fundamental oscillation frequency is calculated from the resonator output and is depicted in Fig. 9(b). Here, it can be seen that highest power is available at a feedback phase of about $\pi/2$ rad.

As a result of this simulation study, the optimal operation point for the MEMS resonator based oscillator circuit has been determined to be at a feedback phase of $\psi_R = \pi/2$ rad. Here, the response is at the maximum of the power-phase curve (Fig. 9(b)) and at the minimum of the frequency-phase curve (Fig. 9(a)), which is both very beneficial. Namely, high power results in a good fundamental harmonic signal content and less effort needed for sustaining vibrations. The minimum in the frequency-phase curve results in little changes in frequency for changes in phase.

To conclude this section, a phase noise plot has been calculated from Fig. 8. This plot is depicted in Fig. 10(a), where the phase noise $\mathcal{L}(\Delta f)$ is expressed in decibels below the carrier per Hertz. For reference, a phase noise plot from [15] for a

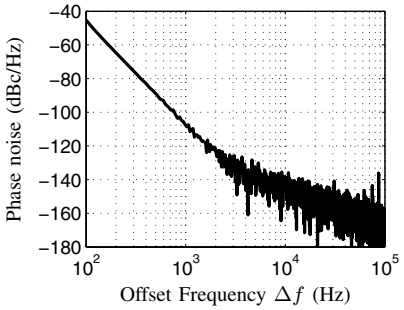

(a) numerical phase noise plot calculated from Fig. 8.

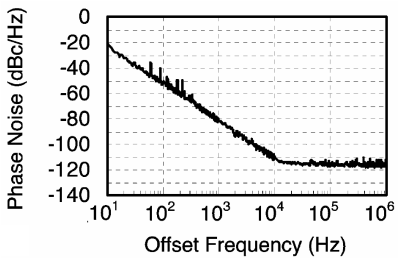

(b) experimental phase noise plot from [15].

Fig. 10. Phase noise plots for a clamped-clamped beam resonator.

clamped-clamped beam resonator with a slightly lower nominal frequency (9.34 MHz) has been depicted in Fig. 10(b). From Fig. 10(a), it can be seen that the narrow peak results in a good phase noise response.

In order to validate the simulation results presented in this section, a following step would consist of experimental validation of the phase feedback principle for MEMS resonators.

V. Conclusion

The principle of phase feedback has been investigated for an oscillator circuit containing a clamped-clamped beam MEMS resonator. By means of simulation studies, it has been shown that phase feedback works very well for this nonlinear MEMS resonator. Phase feedback yields an increase in S/N-ratio of several decades. Frequency-phase curves and power-phase curves are useful for selecting optimal operation points for the phase feedback in oscillator circuits. Simulation results have been found to be very promising. To further understand the concept of phase feedback and to prove the principle in practice, it is highly recommended to experimentally investigate the described approach.

References

[1] C. T.-C. Nguyen, "Vibrating RF MEMS technology: fuel for an integrated micromechanical circuit revolution?" *Transducers '05, Proceedings of the 13th International Conference on Solid-State Sensors, Actuators and Microsystems, June 5–9, Seoul, Korea*, pp. 243–246, 2005.

[2] V. Kaajakari, T. Mattila, A. Oja, and H. Seppä, "Nonlinear Limits for Single-Crystal Silicon Microresonators," *J. Microelectromech. Syst.*, vol. 13, no. 5, pp. 715–724, 2004.

[3] E. A. Gerber and A. Ballato, *Precision Frequency Control; Volume 2: Oscillators and Standards*. Academic Press, London, 1985.

[4] J. R. Vig and A. Ballato, *Ultrasonic Instruments and Devices (Chapter 7: Frequency Control Devices)*. Academic Press, Inc., 1999.

[5] D. Salt, *Hy-Q Handbook of Quartz Crystal Devices*. Van Nostrand Reinhold (UK) Co. Ltd, 1987.

[6] V. Kaajakari, T. Mattila, A. Lipsanen, and A. Oja, "Nonlinear mechanical effects in silicon longitudinal mode beam resonators," *Sensor Actuat. A-Phys.*, vol. 120, no. 1, pp. 64–70, 2004.

[7] J. J. Thomsen, *Vibrations and Stability; Advanced Theory, Analysis and Tools*, 2nd ed. Springer Verlag, Berlin, 2003.

[8] K. Y. Kim and W. Sachse, "Nonlinear Elastic Equation of State of Solids Subjected to Uniaxial Homogeneous Loading," *J. Mater. Sci.*, vol. 35, no. 13, pp. 3197–3205, 2000.

[9] A. H. Nayfeh, *Introduction to Perturbation Techniques*. Wiley-Interscience., 1981.

[10] D. S. Greywall, B. Yurke, P. A. Busch, A. N. Pargellis, and R. L. Willett, "Evading Amplifier Noise in Nonlinear Oscillators," *Phys. Rev. Lett.*, vol. 72, no. 19, pp. 2992–2995, 1994.

[11] B. Yurke, D. S. Greywall, A. N. Pargellis, and P. A. Busch, "Theory of amplifier-noise evasion in an oscillator employing a nonlinear resonator," *Phys. Rev. A*, vol. 51, no. 5, pp. 4211–4229, 1995.

[12] D. S. Greywall, "Sensitive magnetometer incorporating a high-Q nonlinear mechanical resonator," *Meas. Sci. Technol.*, vol. 16, no. 12, pp. 2473–2482, 2005.

[13] R. M. C. Mestrom, R. H. B. Fey, J. T. M. v. Beek, K. L. Phan, and H. Nijmeijer, "Modelling the dynamics of a MEMS resonator: Simulations and experiments," *Sensor Actuat. A-Phys.*, in press.

[14] E. Doedel, A. R. Champneys, T. F. Fairgrieve, Y. A. Kuznetsov, B. Sandstede, and X. Wang, "Auto97: Continuation and bifurcation software for ordinary differential equations (with homcont)," Concordia University, Tech. Rep., 1998.

[15] Y.-W. Lin, S. Lee, S.-S. Li, Y. Xie, Z. Ren, and C. T.-C. Nguyen, "Series-Resonant VHF Micromechanical Resonator Reference Oscillators," *IEEE J. Solid-State Circuits*, vol. 39, no. 12, pp. 2477–2491, 2004.